Enrichment of allelic editing outcomes by Prime Editing in iPS cells

Ryo Niwa[1, 2], Tomoko Matsumoto[1], Alexander Y. Liu[1, 5], Maki Kawato[1], Takayuki Kondo[1, 3, 4], Kayoko Tsukita[1, 3], Haruhisa Inoue[1, 3, 4], Thomas L. Maurissen[1, 6], Knut Woltjen[1]

[1] Center for iPS Cell Research and Application (CiRA), Kyoto University, Kyoto, Japan

[2] Graduate School of Medicine, Kyoto University, Kyoto, Japan

[3] iPSC-Based Drug Discovery and Development Team, RIKEN BioResource Research Center (BRC), Kyoto, Japan

[4] Medical-Risk Avoidance Based On iPS Cells Team, RIKEN Center for Advanced Intelligence Project (AIP), Kyoto, Japan

[5] Present address: School of Biological Sciences, University of California San Diego, CA, USA

[6] Present address: Roche Pharma Research and Early Development, Cardiovascular, Metabolism, Immunology, Infectious Diseases and Ophthalmology, Roche Innovation Center Basel, F Hoffmann-La Roche Ltd., Basel, Switzerland

[*] Correspondence should be addressed to K.W. (woltjen@cira.kyoto-u.ac.jp).

Center for iPS Cell Research and Application (CiRA), Kyoto University

53 Kawahara-cho, Shogoin, Sakyo-ku, Kyoto 606-8507, JAPAN

E-mail: woltjen@cira.kyoto-u.ac.jp

Tel: +81-75-366-7060

Fax: +81-75-366-7079

Abstract

Gene editing in human induced pluripotent stem (iPS) cells with programmable nucleases facilitates reliable disease models, but methods using double-strand break repair often produce random on-target by-products. Prime editing (PE) combines Cas9 nickase with reverse transcriptase (RT) and a prime editing guide RNA (pegRNA) encoding a repair template to reduce by-products. We implemented a GMP-compatible protocol for transfecting Cas9- or PE-2A-mCherry plasmids to track and fractionate human iPS cells based on PE expression level. We compared the editing outcomes of Cas9- and PE-based methods in a GFP-to-BFP conversion assay, at the *HEK3* benchmark locus, and at the *APOE* Alzheimer's risk locus, revealing superior precision of PE at high expression levels. Moreover, sorting cells for PE expression level influenced allelic editing outcomes at the target loci. We expect that our findings will aid in the creation of gene-edited human iPS cells with intentional heterozygous and homozygous genotypes.

Key words:

Prime editing, flow cytometry, FACS, genome editing, iPS cells

Highlights

1. Delivered large plasmids to human iPS cells under GMP-compliant conditions
2. Developed a flow cytometry-based approach to enrich for PE in human iPS cells
3. Demonstrated few on-target indels in cells regardless of PE expression
4. Sorted iPS cells based on PE expression level to influence mono- or bi-allelic editing

Introduction

Human induced pluripotent stem cells (iPS cells) are produced from somatic cells and have indefinite proliferative and differentiation potential[1–3]. In addition, they can differentiate into multiple cell types, while retaining their normal diploid karyotypes and genome from donors. Based on these characteristics, iPS cells are widely used as cellular-level models to study human genetic diseases. Genetic disease modeling is generally achieved by correcting mutations in iPS cells derived from patients with hereditary diseases, or by introducing mutations into iPS cells prepared from healthy donors without diseases[4]. In addition, modifying a target site by deleting, inserting, or replacing specific DNA sequences provides isogenic control cells to study pathogenic variants[5].

Point mutations represent 58% of disease-related polymorphisms registered in the ClinVar database[6]. Precision gene editing technologies are required to reproduce these disease mutations in iPS cells at single nucleotide resolution[7]. The CRISPR-Cas9 system is conventionally used to generate targeted DNA double-strand breaks (DSBs) in the genome, which are subsequently repaired by cellular DNA repair pathways[8,9]. Non-homologous end-joining (NHEJ) results in insertion and deletion (indel) mutations, while microhomology-mediated end-joining (MMEJ) leads to predictable deletions[10]. Both NHEJ and MMEJ are collectively known as mutagenic end-joining (MutEJ), as both repair outcomes lead to the loss or gain of DNA sequence[11]. Typically, to produce specific changes including single nucleotide variants, the homology-directed repair (HDR) pathway is exploited with custom repair templates containing the desired edit, such as double-stranded linear or plasmid DNA, or single-stranded donor oligonucleotides (ssODNs). However, various studies have shown a preference for MutEJ over precise repair by HDR when employing canonical Cas9[12–15].

Variations on Cas9, such as base editing (BE), combine Cas9 nickase (D10A) with a cytidine or adenine deaminase to directly convert specific DNA bases with reduced incidence

of double-strand breaks[6,16]. Although BE can generate precise edits, it is limited to a specific editing window and bases adjacent to the target may be simultaneously converted, resulting in bystander mutations[6]. In contrast, Prime Editing (PE) technology combines Cas9 nickase (H840A) with reverse transcriptase (RT) activity derived from the Moloney murine leukemia virus (M-MLV)[17]. PE utilizes a prime editing guide RNA (pegRNA) with a 3' extension that serves as a reverse transcription template (RTT) and primer binding site (PBS) to incorporate the desired edit. Since prime editing performs everything from single-stranded DNA cleavage to re-writing the genome, editing may be more intentional, and is a breakthrough in genetic disease modeling[18].

This work demonstrates the optimization of PE applications in iPS cells using a GMP-grade electroporation platform. We established a fluorescence-based PE benchmark method by using GFP-to-BFP conversion in iPS cells. To maximize PE efficiency, we developed a strategy of FACS enrichment, in which the PE expression vector was modified with T2A-mCherry, allowing assessment of Prime Editor 2 (PE2) expression levels in cells and their fractionation. The efficiency of our method was benchmarked in iPS cells using *HEK3* and the rs429358 (c.T388C) pathogenic risk variant in *APOE*. Our results demonstrate that the activity of PE increases with the expression level of mCherry, and PE is less mutagenic than the conventional genome-editing method using Cas9. Moreover, our results demonstrate that FACS enrichment can be used to control allelic editing outcomes.

Methods

Human iPS cell culture

409B2 (RIKENBRC #HPS0076), 317-A4 (GFP heterozygously targeted iPS cells), and 317-D6 (GFP homozygously targeted iPS cells)[11,19] were maintained at 37 °C and 5% CO2 in StemFit AK02N medium (Ajinomoto, Cat. No. RCAK02N) on 0.5 mg/mL silk laminin iMatrix-511 (Nippi, Cat. No. 892021) coated 6-well plates or 10 cm dishes. Cell passaging was performed every 7 days during maintenance. The cells were treated with 300 µL or 2 mL of Accumax (Innovative Cell Technologies, Cat. No. AM105-500) in 6-well plates and 10 cm dishes, respectively. The cells were incubated for 10 min at 37 °C to dissociate the cells. Pipetting was performed to detach the cells from the surface and generate a single-cell suspension in 700 µL or 4 mL of medium containing 10 µM ROCK inhibitor, Y-27632 (Wako, Cat. No. 253-00513). Cells were seeded onto iMatrix511-coated plates at a density of 1×10^3 cells/cm^2 in StemFit AK02N medium with 10 µM ROCK inhibitor for 24 h after seeding and then cultured without ROCK inhibitor. All the cell lines were routinely tested for mycoplasma contamination.

Cas9-gRNA vector cloning

The spacer sequence of GFP-targeting gRNA was designed based on a previous work [11]. pSpCas9(BB)-2A-GFP (PX458) was a gift from Feng Zhang (Addgene plasmid # 48138; http://n2t.net/addgene:48138; RRID:Addgene_48138). PX458 was digested by *Eco*RI, and T2A-mCherry was inserted and ligated (KW1013: pSpCas9(BB)-2A-mCherry). The gRNA construct was generated by Golden Gate assembly of annealed oligonucleotides into *the Bbs*I-digested KW1013 plasmid. The oligonucleotides listed in Table 2 were used for gRNA cloning.

Cloning of PE-mCherry constructs

The T2A-mCherry fragment was PCR-amplified from the KW1013 plasmid. pCMV-PE2, a gift from David Liu (Addgene plasmid # 132775; http://n2t.net/addgene:132775; RRID; Addgene_132775), was digested by *Eco*RI and *Pme*I (Thermo Fisher Scientific). The digested product was gel-extracted using the Wizard SV Gel and PCR Clean-Up Kit (Promega). The two fragments were assembled in a single In-Fusion reaction (In-Fusion HD Cloning Kit, Takara, 639650), and the PCR-derived regions of the resulting plasmids were confirmed by sequencing.

pegRNA design and cloning

pU6-pegRNA-GG-acceptor was a gift from David Liu (Addgene plasmid # 132777; http://n2t.net/addgene:132777 ; RRID; Addgene_132777). pegRNA-GFP and pegRNA-APOE were designed using the PrimeDesign web platform version (https://drugthatgene.pinellolab.partners.org/)[20]. The pegRNA construct was generated by Golden Gate assembly of annealed oligonucleotides into the *Bsa*I-digested pU6-pegRNA-GG-acceptor plasmid and sequence verified, as previously reported[17]. The plasmids used in this study are listed in Table 1, and the oligos used for the construction of vectors are listed in Table 2.

Electroporation of plasmids and RNP

For Cas9-based editing, all plasmids for electroporation were prepared using the HiSpeed Plasmid Maxi Kit (Cat. No. 12663), precipitated with ethanol, and dissolved in the MaxCyte electroporation buffer at a concentration of 2.5 μg/μL. For Cas9-based editing, 5 μg of plasmid encoding gRNA-GFP and Cas9 and 5 μg of ssODN repair template (IDT) were mixed in a total volume of 5 μL. The ssODNs used in this study are presented in Table 1. For PE-based editing, 5 μg of the KW1564 vector and 5 μg of the pegRNA-expressing plasmid were mixed in a total volume of 5 μL. Next, 5×10^6 cells resuspended in 50 μL of MaxCyte

electroporation buffer were added to the DNA mixture. The suspension (50 µL) was electroporated into an OC-100□×□2 processing assembly (MaxCyte, Cat. No. SOC-1□×□2) using a MaxCyte STX electroporator (Opt0-5 protocol). Electroporated cells were incubated at 37°C for 30 min and then transferred to an iMatrix511-coated 10 cm dish in StemFit AK02N medium supplemented with 10 µM ROCK inhibitor. Cell preparation for FACS analysis was performed 24 h after electroporation. Otherwise, medium exchange was performed 48 h after electroporation using StemFit AK02N without ROCK inhibitor, and cells were maintained until collection for genotyping on day five or flow cytometry (FC) analysis on day eight. We performed the *APOE* gene editing by ribonucleoprotein (RNP) of Cas9 with NEPA21 following the previously published protocol[11]. APOE gene editing by RNP was performed in T8 iPS cells[21].

Flow cytometry and cell sorting

$5x10^5$ cells were suspended in 1 mL FACS buffer (DPBS supplemented with 2% FBS), and GFP and mCherry fluorescence intensities were analyzed using a BD LSRFortessa Cell Analyzer or BD FACSAria II cell sorter (BD Biosciences) with BD FACSDiva software (BD Biosciences). After setting gates for the singlets, 10,000 events were measured for each population. For editing experiments in 317-A4 iPS cells, the cells were acquired using Pacific Blue (450/50□nm) and FITC (530/30□nm) filters. For cell sorting, cell suspensions were prepared in FACS buffer at a density of 1×10^6 cells/mL and filtered through a 35 µm nylon mesh cap of the tube (Corning, 352235) to remove clumps. Sorting gates were set for the singlet events. The desired population was collected using a BD FACSAria II cell sorter (BD Biosciences) in AK02N medium containing 20 µM Y-27632. Sorting efficiency was confirmed by re-analyzing 300 µL of the media. Raw data were analyzed using FlowJo 10 (FlowJo LLC). Rainbow Calibration Particles (6 peaks) and 3.0 - to 3.4 µm (BD biosciences) were utilized to

171 calibrate the laser strength and determine the sorting gate. The 90 percentiles of the relative
172 mCherry intensity of the unelectroporated cells was defined as the threshold of the mCherry.
173
174 **Genotyping**
175 For genomic DNA extraction, 0.5–1 × 10^6 cells were washed with 1X DPBS, and
176 DNA was purified using the DNeasy Blood & Tissue Kit (Qiagen, Cat. No. 69506) following
177 the manufacturer's protocol. Purified DNA was eluted in 100 µL of AE buffer. Target
178 sequences were amplified by PCR using the KAPA HiFi HS ReadyMix (Kapa Biosystems, Cat.
179 No. KK2602). PCR product cleanup was performed using the ExoSAP-IT Express reagent (Cat.
180 No. 75001) following the manufacturer's protocol, and Sanger sequencing was performed
181 using the BigDye Terminator v3.1 CS Kit (Thermo Fischer Scientific, Cat. No. 4337456). The
182 final product was purified by ethanol precipitation and dissolved in HiDi formamide.
183 Sequencing was performed on a 3500xl Genetic Analyzer (Applied Biosystems). Sequence
184 alignments were analyzed with Snapgene (GSL Biotech LLC), and sequence trace files with
185 low base-calling confidence were excluded manually. The primers used for genotyping are
186 listed in Table 3. Sequencing analysis was performed on mixed sequences using ICE
187 (https://ice.synthego.com/) and DECODR (https://decodr.org/) (REF)[22]. Sequence data from
188 317-A4 iPS cells was used as the reference genome. The parameters were kept at their default
189 values.
190
191 **Droplet digital PCR (ddPCR)**
192 To quantify the APOE 388 mutation created by PE, we prepared a mixture containing
193 10 µL of ddPCR Multiplex Supermix (Bio-Rad, Cat. No. 12005909), 1.8 µL of 20 µM forward
194 and reverse primers each, 1.25 uL of 10 µM APOE-FAM and 0.5 µL of 10 µM hTFRC-HEX
195 probes, and 30 ng of Template DNA, adjusted to a final volume of 20 µL. Droplets were
196 generated using a QX200 Automated Droplet Generator (Bio-Rad). The PCR amplification

197 protocol was as follows: 95°C for 10 min, 40 cycles at 94°C for 30 s and 58°C for 4 min,
198 followed by 98°C for 10 min. The amplified droplets were then read with the QX200 Droplet
199 Reader (Bio-Rad), and data were analyzed using QuantaSoft™ Analysis Pro v1.7.4.
200
201 **Statistical Analysis**
202 The data are presented as the mean ± SD from the indicated numbers of independent
203 experiments and were processed using R 4.0.3, and the R package tidyverse 1.2.0[23] and
204 ggprism[24].
205

Results

GFP to BFP conversion assay to benchmark editing with PE plasmids in iPS cells.

First, we established conditions for PE expression from plasmids in iPS cells. We adopted a GFP-to-BFP conversion assay previously used to optimize ssODN editing[11], where a single amino acid change from tyrosine to histidine (Y66H) in the fluorophore region of GFP is sufficient to convert fluorescent emission of GFP to BFP, and can be quantified in single cells by flow cytometry (Figure 1a)[25]. The pegRNA-GFP was designed to create Y66H, along with a T65S mutation which acts to stabilize BFP, increasing fluorescence by approximately 2-fold[26,27], as well as block the PAM to prevent subsequent re-cleavage of the edited BFP allele (Figure 1b). The spacer sequence is identical to that used in ssODN editing[11]. Conversion to BFP therefore represents the intended PE edit, while MutEJ is detected by loss of fluorescence and unmodified cells remain GFP-positive. These changes were quantified by flow cytometry, resulting in 21.2% editing to BFP in the 317-A4 iPS cell line (monoallelic AAVS1-targeted GFP) with 3 μg of each PE expression plasmid and pegRNAs expression plasmid (Figure 1c).

The PE2 expression vector was modified to couple PE with mCherry using a T2A self-cleaving peptide (PE2-mCherry), such that mCherry expression represents the level of PE expression. Previously, delivery of Cas9 ribonucleoprotein (RNP) and DNA plasmid to human iPS cells was established on the GMP-compliant MaxCyte platform[11,28,29]. However, co-transfection of multiple plasmids in iPS cells has yet to be demonstrated, and we started by optimizing the amount of plasmids by titration. (Figure 1d). We tested the editing efficiency based on the amount of PE-mCherry or pegRNA expressing plasmid (0, 1, 3, and 5 μg), while keeping the second component fixed (5 μg). The proportion of mCherry-positive cells, detected at 24 h after electroporation, indicated transfection efficiency. The proportion of BFP-positive cells on day 7 indicated the amount of correct editing. We confirmed that the increase in mCherry-positive cells correlated with the amount of PE plasmid and the editing efficiency

231 correlated with the amount of pegRNAs plasmid within the titration range. In addition, 5 μg
232 of each plasmid showed consistent transfection efficiency of approximately 83% across
233 multiple electroporations, and we decided to use this condition for the subsequent experiments.
234 Notably, electroporation itself increased the autofluorescence and 31.3% was distinguished as
235 positive when using 90 percentile of electroporated cells as a threshold.
236
237 **FACS enrichment of highly transfected iPS cells to maximize correct editing efficiencies.**
238 Next, we established parameters for FACS enrichment of cells expressing high levels
239 of PE or Cas9. FACS enrichment was performed 24 hours after electroporation. Using
240 fluorescent beads as a calibration ladder for consistency between experiments, the cells were
241 divided into three groups: 'Low', 'Medium' (or 'Med'), and 'High', depending on the level of
242 mCherry expression (Figure 2a). The 90 percentiles of relative mCherry intensity of
243 un-electroporated cells were used as a threshold for the Low population. The mode of each peak
244 of the ladder was first measured, and we defined the mode of the 3rd and 4th peaks as the
245 thresholds for Medium and High populations, respectively. The mCherry expression level
246 varied among the population of transfected iPS cells (Figure 2b, c).
247 The effect of FACS enrichment on the editing outcomes was tested for both PE and
248 ssODN editing (Figure 2c, d). In the total unsorted ('Unsort') population, 33.0% of correct edits
249 were observed for PE, whereas only 1.62% of the correct edits were observed in ssODN editing.
250 MutEJ levels in PE were found to be low (0.993%), while MutEJ was more prevalent than
251 correct edits for ssODN editing (20.3%). In comparison, the ratio of correct edits to MutEJ was
252 0.08 in ssODN editing, as compared to 33.3 in PE. These data verify that PE with plasmids is
253 more efficient and precise than editing with Cas9 and ssODNs in human iPS cells. In the High
254 fraction, on average, 83.6% of iPS cells were converted to BFP by PE while only 18.1%
255 became BFP positive by ssODN. Compared with Unsort, the fold improvement of correct edits
256 by PE were 0.60, 1.90 and 2.50 times in Low, Med, and High fractions, respectively. The fold

improvement by ssODN editing was 0.53, 7.74, and 11.2 times for the respective fractions. Thus, for both PE and ssODN editing, the editing efficiency improved alongside mCherry intensity. Importantly for PE, the proportion of MutEJ only increased 0.43, 1.39, and 1.99 times in the Low, Medium, and High populations compared to Unsort, while in ssODN, MutEJ was increased 1.21, 2.80, and 3.90 times. In the High fractions, MutEJ reached only 18.1% for PE, but 79.2% for ssODN. These data demonstrate that FACS enrichment of PE increases the number of correct edits without a substantial increase in MutEJ, in stark contrast to ssODN editing. These data indicate that PE outcomes may be improved by enrichment using fluorescence, without an increase in MutEJ.

Benchmarking editing efficiencies in iPS cells at endogenous loci.

For benchmarking endogenous gene editing with PE and FACS enrichment, we selected the *HEK3* locus (Figure 2d) that has been used in diverse cell lines such as HEK293T, HeLa, K562, and human embryonic stem (ES) cells[30,31]. This benchmarking pegRNA inserts CTT and caused two detected sequences. Overall, the combination of PE and FACS enrichment resulted in a 3-fold increase in correct edits, reaching 8.0% in the High fraction. MutEJ was undetectable across all fractions by ICE analysis. These data indicate that PE can be improved by fluorescent enrichment at endogenous loci, without co-enrichment of MutEJ.

Evaluation of allelic editing outcomes with FACS enrichment.

Given the potential of iPS cells for modeling genetic diseases, it is important to determine the rate of mono- and biallelic editing at a cellular or clonal population level. We first evaluated allelic editing in 317-D6, a biallelic AAVS1-targeted GFP iPS cell line. In total, six editing patterns are expected (Figure 3a). Since iPS cells with one or two active copies of GFP or BFP only double in their mean fluorescence intensities[19], we recognize that distinguishing between biallelic editing and monoallelic editing with MutEJ is challenging by FACS[11].

However, considering the near-zero proportion of MutEJ generated by PE, we predicted that BFP single-positive iPS cells correspond to biallelic editing, whereas BFP/GFP double-positive iPS cells represent monoallelic editing (Figure 3a). The Unsort population exhibited nearly equal amounts of biallelic (29.4%) and monoallelic (23.1%) editing (Figure 3b). Interestingly, the High population showed more than 3-fold higher biallelic editing (72.6%) than monoallelic editing (22.4%). In the Med population, these proportions were more similar at 43.1% and 36.3% for biallelic and monoallelic edits, respectively. Finally, the Low population reversed this trend, showing nearly half the number of biallelic edits compared to monoallelic editing (7.65% and 14.7%). These results demonstrate that FACS enrichment for defined PE expression levels can skew the outcomes of mono- and biallelic editing at a cellular level.

We then explored the clonal distribution of allelic editing by Cas9 and PE at an endogenous locus. Among the three variants of the apolipoprotein (*APOE*) gene, APOE2, APOE3 (c.C526T, rs7412), and APOE4 (c.T388C, rs429358), APOE4 is associated with the highest risk of Alzheimer's disease (Figure 4a). We therefore chose to engineer the rs429358 APOE3 variant to the APOE4 genotype by both ssODN editing and PE (Figure 4b). Editing by ssODN and Cas9 RNP showed 11.3% correct edits (Figure 4c). However, correct edits were outcompeted by 78.3% +1T insertions. We treated cells with NU7441 (a DNA-PKcs inhibitor), with the aim of depleting +1T insertions and increasing the correct edits (Figure 4d). NU7441 treatment was able to maintain a similar level of correct edits (7.5%). While the decrease in +1T insertion by NU7441 was substantial (55.0%), it was not enough to eliminate it. Next, we created the same variant by PE and FACS enrichment (Figure 4e, f). Sanger sequencing with DECODR software estimated 23.6% APOE4 c.T388C correctly edited alleles in the High fraction, which was validated by droplet digital PCR (ddPCR, 21.3%) (Figure 4f). In contrast, no edits were detected in the Low or Med fractions by Sanger sequencing and DECODR, whereas ddPCR identified 3% and 8% correct edits, respectively (Figure 4f). MutEJ was not discernible in any of the fractions by Sanger sequencing analyzed by DECODR.

Finally, we determined the number of APOE4 biallelic and monoallelic edited iPS cells at a clonal level (Figure 4g). Using Cas9 RNP, two bi- and nine monoallelically edited clones were obtained, however, 8 of the monoallelically edited clones were accompanied by a +1 insertion in other alleles. Using PE, the Med and Low populations yielded only monoallelic clones (1 and 8, respectively), with many unedited clones. From the High PE condition, we isolated twenty-four mono- and one biallelically edited colony. Moreover, no unintended edits were confirmed by Sanger sequencing of clones. Collectively, these findings suggest that a combination of PE and FACS enrichment can fulfill a crucial need in establishing an allelic series of isogenic iPS cells for disease modeling.

Discussion

In this research, we demonstrate the superior efficiency and precision of PE over Cas9-based ssODN editing in iPS cells. Also, applying FACS, we successfully enriched cells exhibiting varied editing efficiencies. Leveraging a GFP to BFP reporter assay with single-cell resolution, our findings revealed that PE generated notably fewer MutEJ events compared to ssODN editing. Finally, we show that FACS enrichment can modulate the frequency of mono- or bi-allelic editing, demonstrating its utility in controlling allelic editing outcomes.

The GMP-approved MaxCyte platform has been used for plasmid transfection into T cells, HEK293T cells, and CHO cells[32,33]. Previous research used the MaxCyte to successfully introduce plasmid, mRNA, and RNPs into iPS cells[11,28,29,34]. As iPS cells hold significant promise not only for disease modeling but also for genome-edited cellular regenerative medicine anticipating ex vivo applications for cell therapy, our findings are of paramount importance.

Our protocol demonstrates a highly reproducible FACS gating strategy through the implementation of a fluorescent bead ladder. FACS provides advantages for PE editing using plasmid vectors by eliminating non-transfected cells and isolating cells based on their expression level. Our FACS enrichment data also indicate that PE activity was underestimated in the unsorted population, similar to a previous study on the combination of Cas9 and FACS enrichment reported[35]. Another study employed *piggyBac* transposition to introduce PE into iPS cells for long-term stable expression, yet observed no increase in editing over 40 days of continuous expression[36], suggesting that the effects of PE are realized early after transfection. Using FACS enrichment, it is possible to select cells with modest PE expression for editing with high efficiency pegRNAs (such as pegRNA-GFP), and high PE expression for editing with low efficiency pegRNAs (such as pegRNA-APOE).

To bias the reaction of heteroduplex removal in the PE repair step, a second nicking guide RNA (ngRNA) can be used to nick approximately 50 bases in the editing region. Prime

editing with the ngRNA used is called PE3[16,17,37]. Although previous studies have shown that PE3 can be further improved by additional nicking, this also increases MutEJ. Also, using multiple gRNA including pegRNA in a single experiment increases the sites experimentalists require to confirm off-target activity. Thus, our study focused on PE2. Editing of GFP was found to be efficient; however, editing at endogenous loci was variable. PE3 can be a powerful method for improving editing efficiency. Furthermore, in PE, almost all edits were targeted edits. Previous studies have shown that PE is less likely to occur in cells with mature Mismatch Repair (MMR) such as iPS cells[30]. PE4 is a method in which the transient expression of a dominant-negative MMR protein (MLH1dn) is combined with PE2. This temporal inhibition of MMR showed the potential to increase editing efficiency in iPSCs[38]. Combined with FACS enrichment, this method may enable further flexible and accurate genome editing.

Even without FACS, we observed a significant disparity in by-products between ssODN editing and PE. Upon FACS enrichment, ssODN editing showed a marked increase in the proportion of MutEJ accompanied by HDR, whereas, in PE, only the proportion of correct edits surged. This disparity is caused by the increased likelihood of DSBs due to elevated Cas9 expression levels, whereas PE's nick-based editing mechanism enhances mainly the rate of correct editing over MutEJ. While our observations were consistent for editing a single nucleotide variant in the *APOE* gene, we cannot guarantee that similar patterns would be observed for other genes or pegRNA and mutation designs without a genome-wide effort. In addition, pegRNA activity differs between *GFP* and *APOE*. This resulted in high Bi-allelic editing in *GFP*, whereas high Mono-allelic editing was observed in *APOE*. Allelic editing may require a high level of PE activity.

Conclusion

Combination of PE and FACS enrichment allows highly efficient and accurate gene editing. The combined protocol is a useful method, as the accuracy of PE does not lead to a significant increase in by-products. Also, fractionation by FACS based on PE expression level can influence mono- or bi-allelic editing. Improving the reliability of gene editing outcomes will greatly facilitate the generation of genetic disease models and possibly therapies using human iPS cells.

Acknowledgment

We thank Suji Lee for technical assistance in cell culture and molecular biology, Dr. Kanae Mitsunaga for helping establish conditions for FACS analysis and cell sorting, and Dr. Peter Gee for helping establish conditions for large plasmid delivery on the MaxCyte and reviewing the manuscript. We thank Dr. Ryo Yamada for his mentorship and guidance of R.N. as part of the Medical Innovation Program and providing the inspiration for statistical methods applied to FACS.

Funding information

R.N. is a trainee of the Medical Innovation Program managed by Kyoto University and supported by JST SPRING (Grant Number JPMJSP2110). This study was supported by funding to K.W. from the Japan Agency for Medical Research and Development (AMED) for the Core Center for iPS Cell Research (Grant Number JP21bm0104001), the Core Center for Regenerative Medicine and Cell and Gene Therapy (Grant Number JP23bm1323001), the COVID-19 Private Fund (Shinya Yamanaka, CiRA, Kyoto University), and the Canadian National Research Council.

Competing Interest Statement

The authors declare that they have no conflicts of interest.

Author contribution

RN: Conceptualization, Formal analysis, Investigation, Resources, Writing - Original Draft, Writing - Review & Editing, Visualization

TM: Methodology, Investigation, Resources

AYL: Investigation, Resources

MK: Investigation

404 TK: Investigation, Resources

405 KT: Resources

406 HI: Investigation, Resources

407 TLM: Conceptualization, Investigation, Writing - Review & Editing

408 KW: Conceptualization, Formal analysis, Investigation, Resources, Writing - Original Draft,

409 Writing - Review & Editing, Supervision, Project administration, Funding acquisition

410

References

1. Takahashi K, Tanabe K, Ohnuki M, et al. Induction of Pluripotent Stem Cells from Adult Human Fibroblasts by Defined Factors. Cell 2007;131(5):861–872; doi: 10.1016/j.cell.2007.11.019.
2. Hsu PD, Scott DA, Weinstein JA, et al. DNA targeting specificity of RNA-guided Cas9 nucleases. Nat Biotechnol 2013;31(9):827–832; doi: 10.1038/nbt.2647.
3. Shi Y, Inoue H, Wu JC, et al. Induced pluripotent stem cell technology: a decade of progress. Nat Rev Drug Discov 2017;16(2):115–130; doi: 10.1038/nrd.2016.245.
4. Rowe RG, Daley GQ. Induced pluripotent stem cells in disease modelling and drug discovery. Nat Rev Genet 2019;20(7):377–388; doi: 10.1038/s41576-019-0100-z.
5. Nami F, Ramezankhani R, Vandenabeele M, et al. Fast and Efficient Generation of Isogenic Induced Pluripotent Stem Cell Lines Using Adenine Base Editing. The CRISPR Journal 2021;4(4):502–518; doi: 10.1089/crispr.2021.0006.
6. Rees HA, Liu DR. Base editing: precision chemistry on the genome and transcriptome of living cells. Nat Rev Genet 2018;19(12):770–788; doi: 10.1038/s41576-018-0059-1.
7. Kim S-I, Matsumoto T, Kagawa H, et al. Microhomology-assisted scarless genome editing in human iPSCs. Nat Commun 2018;9(1):939; doi: 10.1038/s41467-018-03044-y.
8. Mali P, Yang L, Esvelt KM, et al. RNA-Guided Human Genome Engineering via Cas9. Science 2013;339(6121):823–826; doi: 10.1126/science.1232033.
9. Sander JD, Joung JK. CRISPR-Cas systems for editing, regulating and targeting genomes. Nat Biotechnol 2014;32(4):347–355; doi: 10.1038/nbt.2842.
10. Ceccaldi R, Rondinelli B, D'Andrea AD. Repair Pathway Choices and Consequences at the Double-Strand Break. Trends in Cell Biology 2016;26(1):52–64; doi: 10.1016/j.tcb.2015.07.009.
11. Maurissen TL, Woltjen K. Synergistic gene editing in human iPS cells via cell cycle and DNA repair modulation. Nat Commun 2020;11(1):2876; doi: 10.1038/s41467-020-16643-5.
12. Howden SE, McColl B, Glaser A, et al. A Cas9 Variant for Efficient Generation of Indel-Free Knockin or Gene-Corrected Human Pluripotent Stem Cells. Stem Cell Reports 2016;7(3):508–517; doi: 10.1016/j.stemcr.2016.07.001.
13. Idoko-Akoh A, Taylor L, Sang HM, et al. High fidelity CRISPR/Cas9 increases precise monoallelic and biallelic editing events in primordial germ cells. Sci Rep 2018;8(1):15126; doi: 10.1038/s41598-018-33244-x.
14. Miyaoka Y, Berman JR, Cooper SB, et al. Systematic quantification of HDR and NHEJ reveals effects of locus, nuclease, and cell type on genome-editing. Sci Rep 2016;6(1):23549; doi: 10.1038/srep23549.

15. Hussmann JA, Ling J, Ravisankar P, et al. Mapping the genetic landscape of DNA double-strand break repair. Cell 2021;184(22):5653-5669.e25; doi: 10.1016/j.cell.2021.10.002.
16. Anzalone AV, Koblan LW, Liu DR. Genome editing with CRISPR–Cas nucleases, base editors, transposases and prime editors. Nat Biotechnol 2020;38(7):824–844; doi: 10.1038/s41587-020-0561-9.
17. Anzalone AV, Randolph PB, Davis JR, et al. Search-and-replace genome editing without double-strand breaks or donor DNA. Nature 2019;576(7785):149–157; doi: 10.1038/s41586-019-1711-4.
18. Schene IF, Joore IP, Oka R, et al. Prime editing for functional repair in patient-derived disease models. Nat Commun 2020;11(1):5352; doi: 10.1038/s41467-020-19136-7.
19. Oceguera-Yanez F, Kim S-I, Matsumoto T, et al. Engineering the AAVS1 locus for consistent and scalable transgene expression in human iPSCs and their differentiated derivatives. Methods 2016;101:43–55; doi: 10.1016/j.ymeth.2015.12.012.
20. Hsu JY, Grünewald J, Szalay R, et al. PrimeDesign software for rapid and simplified design of prime editing guide RNAs. Nat Commun 2021;12(1):1034; doi: 10.1038/s41467-021-21337-7.
21. Kondo T, Hara N, Koyama S, et al. Dissection of the polygenic architecture of neuronal Aβ production using a large sample of individual iPSC lines derived from Alzheimer's disease patients. Nat Aging 2022;2(2):125–139; doi: 10.1038/s43587-021-00158-9.
22. Conant D, Hsiau T, Rossi N, et al. Inference of CRISPR Edits from Sanger Trace Data. The CRISPR Journal 2022;5(1):123–130; doi: 10.1089/crispr.2021.0113.
23. Wickham H, Averick M, Bryan J, et al. Welcome to the Tidyverse. JOSS 2019;4(43):1686; doi: 10.21105/joss.01686.
24. Dawson C. Csdaw/Ggprism: Ggprism 1.0.2. 2021; doi: 10.5281/ZENODO.4556067.
25. Heim R, Prasher DC, Tsien RY. Wavelength mutations and posttranslational autoxidation of green fluorescent protein. Proc Natl Acad Sci USA 1994;91(26):12501–12504; doi: 10.1073/pnas.91.26.12501.
26. Joly E. Optimising Blue Fluorescent Protein (BFP) for use as a mammalian reporter gene in parallel with Green Fluorescent Protein (GFP). Nat Prec 2007; doi: 10.1038/npre.2007.1259.1.
27. Glaser A, McColl B, Vadolas J. GFP to BFP Conversion: A Versatile Assay for the Quantification of CRISPR/Cas9-mediated Genome Editing. Molecular Therapy - Nucleic Acids 2016;5:e334; doi: 10.1038/mtna.2016.48.
28. Kagita A, Lung MSY, Xu H, et al. Efficient ssODN-Mediated Targeting by Avoiding Cellular Inhibitory RNAs through Precomplexed CRISPR-Cas9/sgRNA Ribonucleoprotein. Stem Cell Reports 2021;16(4):985–996; doi: 10.1016/j.stemcr.2021.02.013.

29. Roig-Merino A, Urban M, Bozza M, et al. An episomal DNA vector platform for the persistent genetic modification of pluripotent stem cells and their differentiated progeny. Stem Cell Reports 2022;17(1):143–158; doi: 10.1016/j.stemcr.2021.11.011.

30. Chen PJ, Hussmann JA, Yan J, et al. Enhanced prime editing systems by manipulating cellular determinants of editing outcomes. Cell 2021;184(22):5635-5652.e29; doi: 10.1016/j.cell.2021.09.018.

31. Adikusuma F, Lushington C, Arudkumar J, et al. Optimized nickase- and nuclease-based prime editing in human and mouse cells. Nucleic Acids Research 2021;49(18):10785–10795; doi: 10.1093/nar/gkab792.

32. Gee P, Lung MSY, Okuzaki Y, et al. Extracellular nanovesicles for packaging of CRISPR-Cas9 protein and sgRNA to induce therapeutic exon skipping. Nat Commun 2020;11(1):1334; doi: 10.1038/s41467-020-14957-y.

33. Bozza M, De Roia A, Correia MP, et al. A nonviral, nonintegrating DNA nanovector platform for the safe, rapid, and persistent manufacture of recombinant T cells. Sci Adv 2021;7(16):eabf1333; doi: 10.1126/sciadv.abf1333.

34. Xu H, Kita Y, Bang U, et al. Optimized electroporation of CRISPR-Cas9/gRNA ribonucleoprotein complex for selection-free homologous recombination in human pluripotent stem cells. STAR Protocols 2021;2(4):100965; doi: 10.1016/j.xpro.2021.100965.

35. Lonowski LA, Narimatsu Y, Riaz A, et al. Genome editing using FACS enrichment of nuclease-expressing cells and indel detection by amplicon analysis. Nat Protoc 2017;12(3):581–603; doi: 10.1038/nprot.2016.165.

36. Eggenschwiler R, Gschwendtberger T, Felski C, et al. A selectable all-in-one CRISPR prime editing piggyBac transposon allows for highly efficient gene editing in human cell lines. Sci Rep 2021;11(1):22154; doi: 10.1038/s41598-021-01689-2.

37. Chen PJ, Liu DR. Prime editing for precise and highly versatile genome manipulation. Nat Rev Genet 2022; doi: 10.1038/s41576-022-00541-1.

38. Bonnycastle LL, Swift AJ, Mansell EC, et al. Generation of Human Isogenic Induced Pluripotent Stem Cell Lines with CRISPR Prime Editing. The CRISPR Journal 2024;7(1):53–67; doi: 10.1089/crispr.2023.0066.

Figure Legends

Figure 1. GFP-to-BFP conversion assay to optimize plasmid delivery of PE in human iPS cells using the MaxCyte platform

(a) Schematic overview of editing outcomes in heterozygous GFP reporter iPS cells (317-A4). A schematic of the Flow Cytometry (FC) distribution plot indicates each population. (b) Design of the pegRNA-GFP used in this study. The spacer sequence is indicated by a green arrow and the nicking position is indicated by the triangle. ssODN editing with Cas9 uses the same protospacer sequence[11]. RTT and PBS sequences are indicated by blue underlines. The PAM is in bold. Nucleotide changes leading to BFP are indicated in blue characters. (c) Representative plot of FACS analysis after GFP-to-BFP conversion. (d) Titration of PE2-mCherry (left) and pegRNA-GFP (right) plasmids. 'mCherry positive' indicates the proportion of cells over the 90 percentile of mCherry intensity in non-transfected cells at 24hrs after electroporation. 'Correct edit' indicates the proportion of BFP-converted cells on day 7 after electroporation.

Figure 2. FACS enrichment to maximize PE or ssODN editing efficiency

(a) Schematic of FACS approach to cell fractionation based on transfection and expression level. Gating scheme was derived from a fluorescent calibration bead ladder and a representative histogram of mCherry positive cells with sorting gates. (c) Gating scheme and quantification of editing outcomes using Cas9-mCherry and ssODN-GFP. (d) Gating scheme and quantification of editing outcomes using PE and pegRNA-GFP. All data in (c, d) are presented as the mean ± S.D. of three technical replicates of independent electroporations for each condition. (e) Design of pegRNA-HEK3 and editing outcomes as measured by Sanger sequencing.

Figure 3. Modulating the allelic editing outcomes by FACS enrichment

(a) Schematic of the expected GFP editing outcomes in a homozygous AAVS1-CAG::GFP iPS cell line. (b) Allelic editing outcomes following FACS enrichment (N=3). Each fractioned population showed different pattern in editing outcomes.

Figure 4. APOE gene editing to recreate a disease model for Alzheimer's disease in iPS cells

(a) Table of APOE risk variant alleles for Alzheimer's disease. (b) Schematic of the design for gRNA- and pegRNA-APOE. (c) TIDE plot of ssODN editing in T8 iPS cells. (d) ssODN editing with NU7441 to reduce +1 insertion. (e, f) Quantification of Correct edits by DECODR analysis (e) and ddPCR (f) in 317-A4 iPS cells after PE and mCherry FACS. (g) Clonal distribution of gene editing outcomes at the APOE locus using ssODN or PE.

Table 1. Plasmids used in this study

Table 2. Oligos used for vector construction in this study

Table 3. Primers used for genotyping and sequence analysis

Table 4. crRNA and ssODN used in this study

558 **Table 1. Plasmids used in this study**

Purpose	**Plasmid ID**	**Plasmids**
ssODN editing	KW1013	pSpCas9(BB)-2A-mCherry
ssODN editing	KW1322	pSpCas9(BB)-2A-mCherry-GFP
PE	KW1564	pCMV-PE2-T2A-mCherry
PE	KW1548	pU6-pegRNA-GFP
PE	Addgene#132778	U6-pegRNA-HEK3-ins3 (Anzalone *et al*., 2019)
PE	KW1573	pU6-pegRNA-GG-ApoE

559

560 **Table 2. Oligos used for vector construction in this study**

Oligo ID	Length	Sequence	Content
dna2935	24	caccGCTGAAGCACTGCACGCCGT	sgRNA-GFP-s
dna2936	24	aaacACGGCGTGCAGTGCTTCAGC	sgRNA-GFP-as
dna3433	29	caccGCTGAAGCACTGCACGCCGTgtttt	pegRNA-GFP-spacer-s
dna3434	29	ctctaaaacACGGCGTGCAGTGCTTCAGC	pegRNA-GFP-spacer-as
dna3435	30	gtgcACCCTGAGCCACGGCGTGCAGTGCTT	pegRNA-GFP-ext-s
dna3436	30	aaaaAAGCACTGCACGCCGTGGCTCAGGGT	pegRNA-GFP-ext-as
dna3559	30	caccgCGCCGCGGTACTGCACCAGGgtttt	APOE_Spacer_s
dna3560	30	ctctaaaacCCTGGTGCAGTACCGCGGCGc	APOE_Spacer_as
dna3561	31	gtgcGTGcGCGGCCGCCTGGTGCAGTACCGC	APOE_Normal_s
dna3562	31	aaaaGCGGTACTGCACCAGGCGGCCGCgCAC	APOE_Normal_as

561

562

563

564 **Table 3. Primers used for genotyping and sequence analysis**

Sequencing	Primer ID	Sequence
GFP	dna549	AGCAAGGGCGAGGAGCTGTT
	dna649	GCCGTTCTTCTGCTTGTCGG
HEK3	dna3449	ATGTGGGCTGCCTAGAAAGG
	dna3450	CCCAGCCAAACTTGTCAACC
APOE	dna3244	GGCGCTGATGGACGAGACCA
	dna3241	CACACAGACACAGATGGAGAG

565

566

Table 4. ssODN used in this study

ssODN ID	ssODN name	Sequence
ss027	eGFPc.194G.196C-50/50-t	CGGCAAGCTGCCCGTGCCCTGGCCCACCC TCGTGACCACCCTGAgCcACGGCGTGCAG TGCTTCAGCCGCTACCCCGACCACATGAA GCAGCACGACTTC
ss021	APOE-rs429358-C[e4]	GGCCGAGCATGGCCTGCACCTCGCCGCGG TACTGCACCAGGCGGCCGCGCACGTCCTC CATGTCCGCGCCCAGCCGGGCCTGCGCCG CCTGCAGCTCCTT
rna059	APOE-x386-e3	/AlTR1/rGrCrGrGrArCrArUrGrGrAr GrGrArCrGrUrGrUrGrGrUrUrUrUrAr GrArGrCrUrArUrGrCrU/AlTR2/

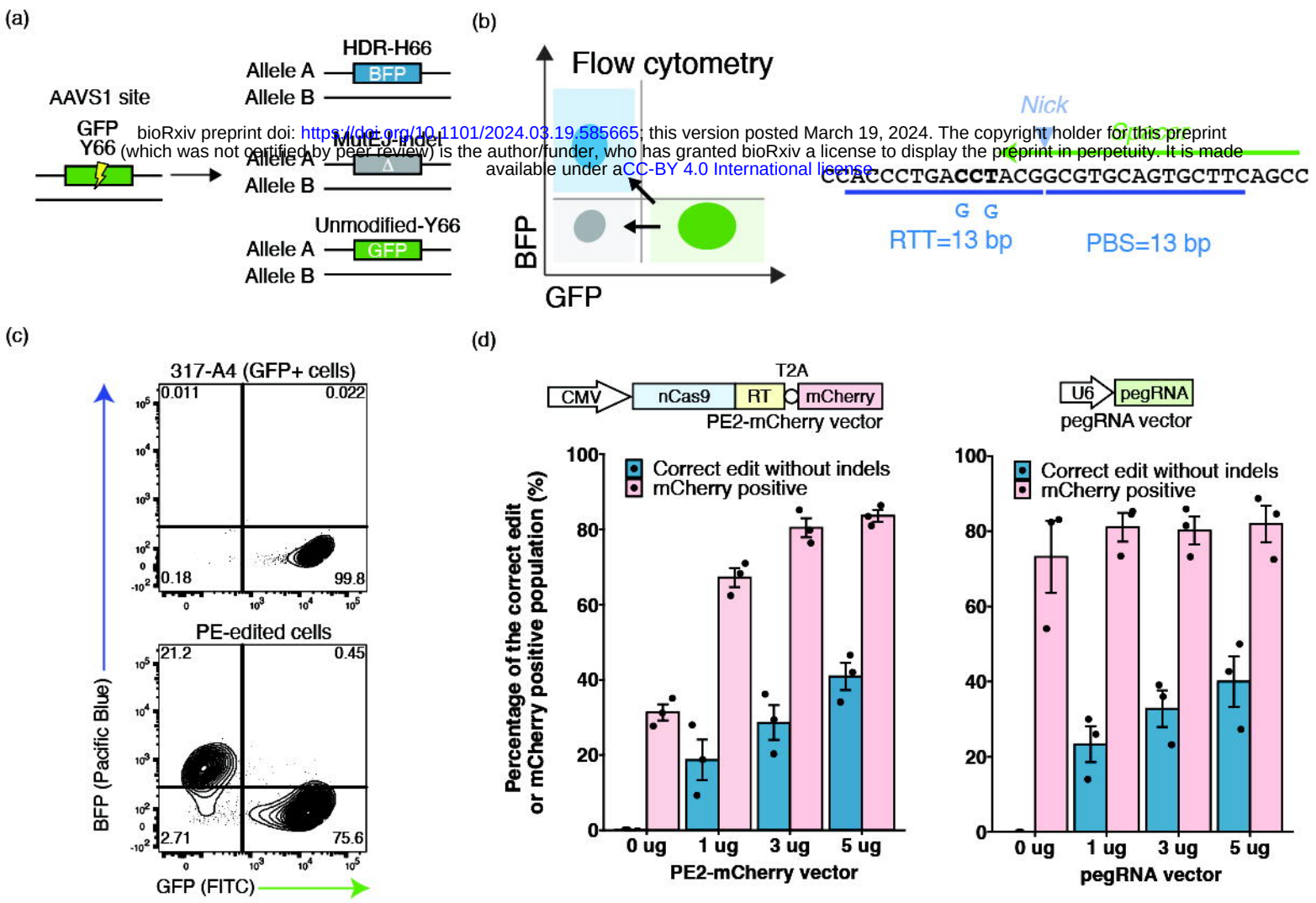

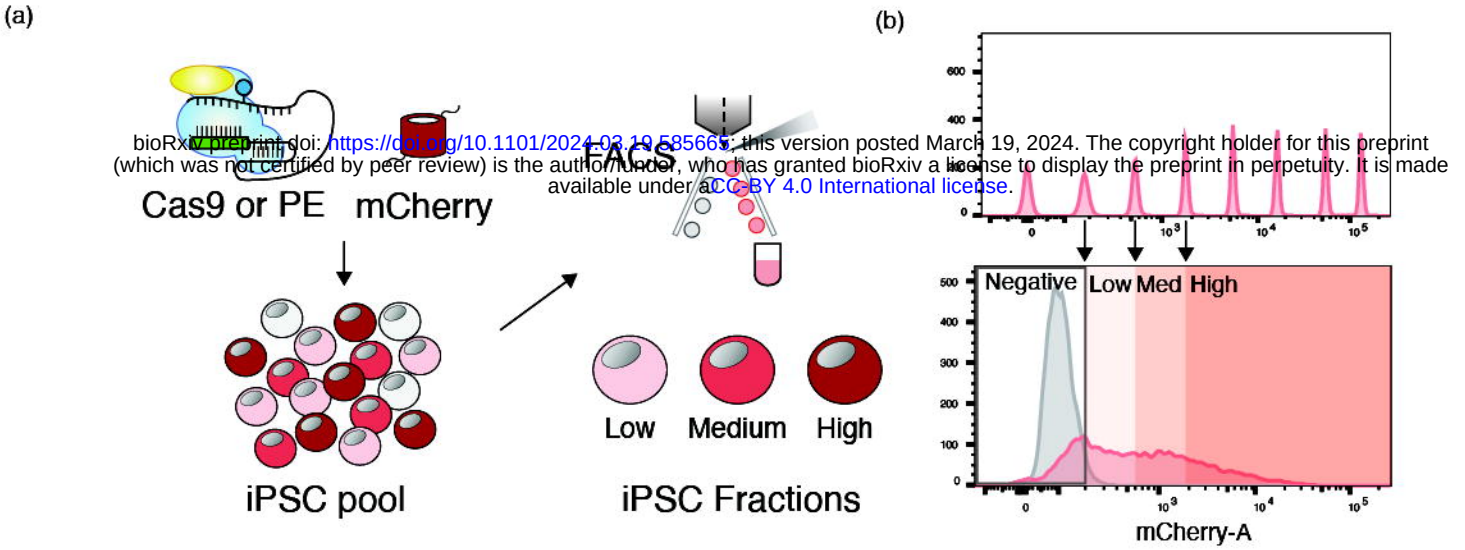

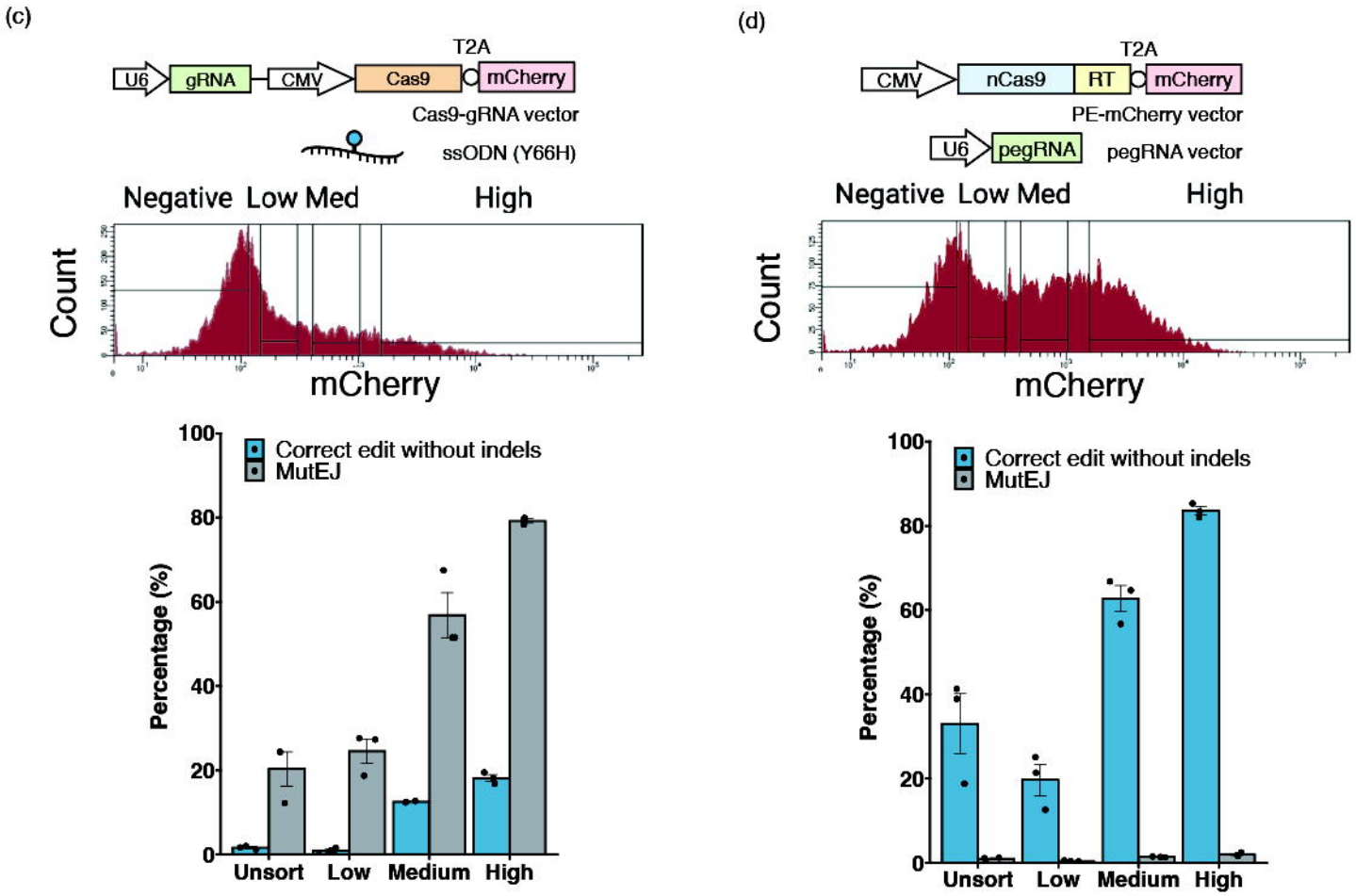

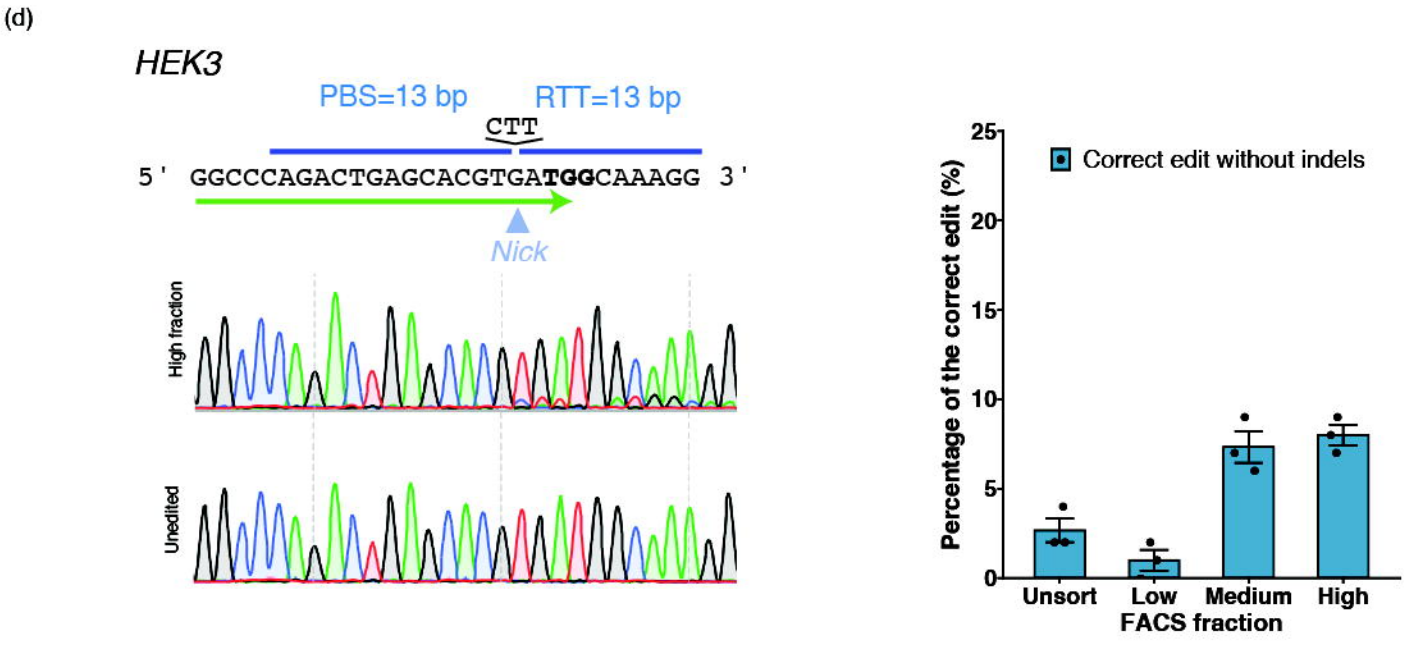

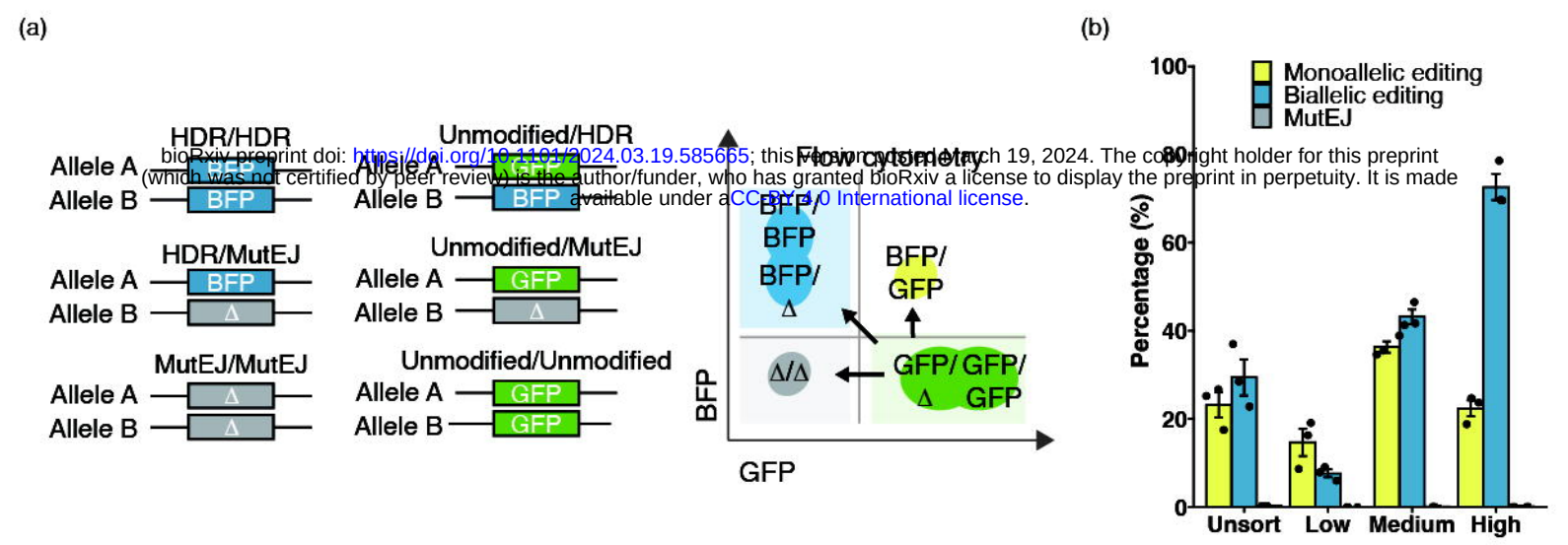

(a)

	rs429358 (c. T388C)	rs7412 (c. C526T)	APOE risk
APOE2	T	T	3rd
APOE3	T	C	2nd
APOE4	C	C	1st

(b)

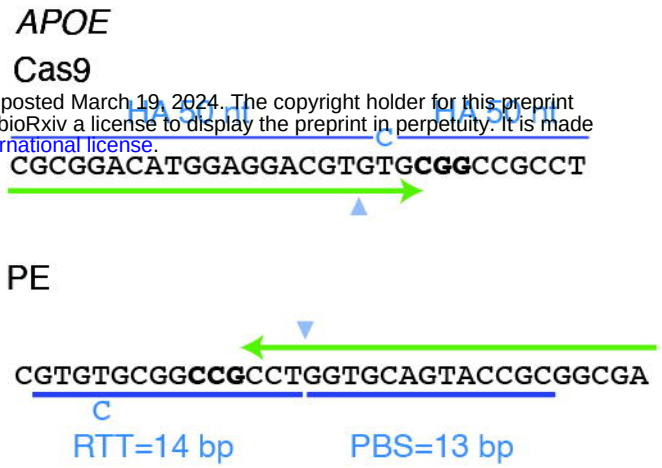

(c)

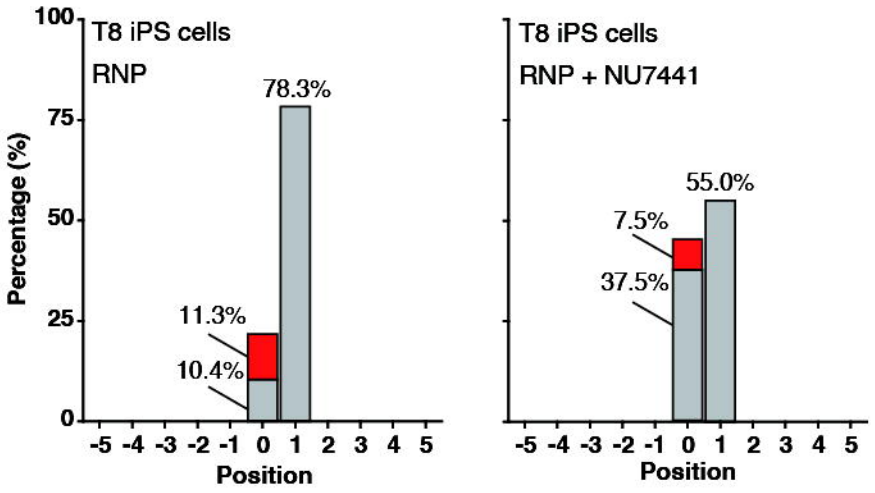

(d)

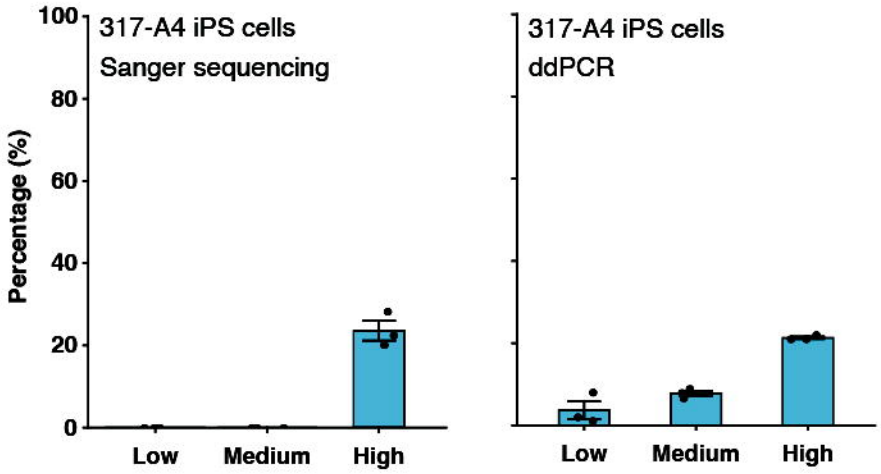

(e)